

Color Diffusion Model for Active Contours - An Application to Skin Lesion Segmentation

Mihai Ivanovici and Diana Stoica

Abstract—Most of the existing diffusion models are defined for gray-scale images. We propose a diffusion model for color images to be used as external energy for active contours. Our diffusion model is based on the first-order moment of the correlation integral expressed using ΔE distances in the CIE Lab color space. We use a multi-scale approach for active contours, the diffusion being independently computed at various scales. We validate the model on synthetic images, including multi-fractal color textures, as well as medical images representing melanoma. We conclude that the proposed diffusion model is valid for use in skin lesion segmentation in color images using active contours.

I. INTRODUCTION

Active contours were introduced in 1988 by Kass, Witkin and Terzopoulos [1] and they are defined as energy-minimizing curves guided by various forces, gradually advancing towards edges in the analyzed image. The active contours are successfully and widely used for image segmentation in medical applications [2], especially for computed tomography and brain magnetic resonance imaging. In this paper we use the active contours to perform the segmentation of skin lesions, such as melanoma or psoriasis, in dermatological color images.

The initial active contour is incrementally deformed according to several specified energies. According to the original definition, an active contour is a spline $c(s) = [x(s), y(s)]$, with $s \in [0, 1]$, that minimizes the following energy equation [3]:

$$\varepsilon(c) = \varepsilon_{int}(c) + \varepsilon_{ext}(c) = \int_0^1 [E_{int}(c) + E_{ext}(c)] ds \quad (1)$$

where $c = c(s)$, $\varepsilon_{int}(c)$ represents the total *internal* energy and $\varepsilon_{ext}(c)$ represents the total *external* energy along the contour c . The internal energy is intrinsic to the spline and the external energies comes usually from the image data. The internal energy ε_{int} is usually written as:

$$\varepsilon_{int}(c) = \int_0^1 \frac{1}{2} [\alpha(s) |c'(s)|^2 + \beta(s) |c''(s)|^2] ds \quad (2)$$

where $c'(s)$ and $c''(s)$ are the first and the second derivatives, weighted by $\alpha(s)$ and $\beta(s)$ which are usually two constants determined empirically.

Xu [4] identifies several issues of the original model [1], including the fact that the initialization of the contour has

to be close to the edge of interest. Those were partially addressed in the original article [1] by using the propagation in the scale space, further described in [5] [6]. The placement of the active contour very close to the edges was solved by using multi-resolution methods [7], pressure forces [8] or distance potentials [9]. The basic idea is to increase the capture domain, so that the active contour could be attracted from a larger distance.

There are several attempts to extend the active contour approach to color images, by proposing various diffusion models for multi-dimensional data. In [10] the external energy is a weighted mixture of image color contrast and intensity. The foveal wavelets are used in [11] and the squared local contrast in the context of a principal component analysis in [12], both of them being based on extensions of the now-classical di Zenzo gradient for multi-valued data [13].

In this paper we propose a new diffusion model for color images. The external energy forces that drive the active contours are given by the mean CIE Lab ΔE distance computed locally at different resolutions for the original color image. We validate our model in the framework of a multi-scale active contour approach, using synthetic color images. Then we present our results on melanoma image segmentation and conclude this paper.

II. COLOR DIFFUSION MODEL

The correlation integral is used in [14] for the computation of the correlation dimension, which is a variant of the fractal dimension [15]. The fractal dimension, which is a measure of complexity, is widely used for texture characterization. The correlation integral $C(r)$ for a set of points $\{X_1, X_2, \dots, X_N\}$ is defined as:

$$C(r) = \lim_{N \rightarrow \infty} \frac{2q}{N(N+1)} \quad (3)$$

where q is the number of pairs (i, j) whose distance $|X_i - X_j|$ is less than r . Basically, the correlation integral is a cumulative density function for all the distances between the elements of the set.

Starting from this definition, we propose a diffusion model for color images based on the first order moment of the correlation integral. For a certain resolution n , the value of one point (x, y) in the energetic surfaces is given by the mean color distance computed in a neighborhood of size $n \times n$ centered in that specific point. If we consider the pixels p_i in the $n \times n$ vicinity as placed in a vector of size n^2 , we

*The authors are with MIV Imaging Venture Laboratory, Department of Electronics and Computers, Transilvania University, Braşov, România. Contact e-mail: mihai.ivanovici at unitbv.ro

have to compute the average value of $\frac{n^2(n^2-1)}{2}$ distances d between any two pixel values:

$$E_{\text{ext}}(x, y)|_{n \times n} = \frac{2}{n^2(n^2-1)} \sum_{i=1}^{n^2-1} \sum_{j=i+1}^{n^2} d(p_i, p_j) \quad (4)$$

For the distance between pixel colors we used the CIE Lab ΔE distance, therefore the external energy forces that drive the active contours are given by the mean CIE Lab ΔE distance computed locally at different resolutions, based on the original image. The CIE Lab color space was created as an attempt to linearize the perception of color differences, therefore the color distance associated, called ΔE , is an Euclidean distance. For two color values $p_1 = (L_1, a_1, b_1)$ and $p_2 = (L_2, a_2, b_2)$, the distance $d(p_1, p_2) = \Delta E$ where

$$\Delta E = \sqrt{(L_1 - L_2)^2 + (a_1 - a_2)^2 + (b_1 - b_2)^2} \quad (5)$$

Being related to the fractal dimension, the first-order moment of the correlation dimension represents a measure of the local heterogeneity of a texture, in a certain neighborhood at a given resolution. Such a measure will definitely emphasize the ruptures between two different textures and implicitly the delimiting edges. In our case, the concept of diffusion is based on the low-pass filtering behavior of the computation of texture complexity in a sliding window, ensuring the required monotony (see also Section IV on approach validation).

III. THE ACTIVE CONTOUR FRAMEWORK

In order to prove the validity and the usefulness of our diffusion model, we used a multi-scale active contour approach [16]. For a given image, we compute several pseudo-images that represent the mean CIE Lab ΔE distance of the image at different resolutions, i.e. computed with various window sizes. Initially, the points of the active contour start to move on the energy surface given by the mean distance computed in large windows (e.g. 75×75 pixels) and, as the points advance, they use (and jump to) the potential energy given by the mean distance computed in smaller windows, until the final active contour *crawls* on the mean distance computed in a 3×3 window.

The points of the active contour move on a certain energy surface as long as the difference between the potential energy of the current surface and the next one monotonously increases (see Figure 1 for an illustration of energy curves at different scales - the blue curve for the largest and the red curve for the smallest, corresponding to an ideal rectangular impulse (with black); an initial point of the active contour is marked as a square and the arrows indicate its evolution, as it advanced towards the final edge). When that difference starts to diminish (i.e. an indication that the next mean distance surface has enough energy to drive the points of the active contour), the points of the active contour will use the next mean distance surface, and so on. The active contour will stop when it reaches a plateau on the mean distance curve

computed with the smallest window, i.e. the closest to the final contour. In addition, the points of the active contour independently move on the mean ΔE surfaces in order to ensure the rapid convergence of the algorithm towards the final solution [16]. In our implementation we have used 21 window sizes - the odd sizes from 3 to 35, plus 45, 55, 65 and 75 for the generation of color diffusions.

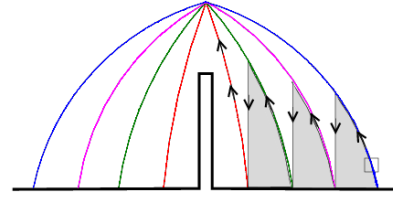


Fig. 1. How potential energy is used by the points of the active contour.

IV. APPROACH VALIDATION

In the context of our application of skin lesion segmentation, the hypothesis that we make is that in medical images there are two types of textures, exhibiting different complexities: one corresponding to the healthy skin and the other to the lesion (the complexity of the latter one being usually larger). Roughly speaking, the healthy skin is relatively homogeneous, compared to the heterogeneous surface of a melanoma or psoriasis lesion.

For a synthetic test image with two regions of different colors we obtain the diffusions at various resolutions, as shown in Figure 2. The middle horizontal line of every diffusion image, i.e. energy surface, is represented in Figure 3 as a potential energy curve, illustrating how the computed mean ΔE distance plays the role of a potential energy. For the ideal sharp edges of a theoretical rectangular impulse, the monotony property required by a diffusion model is evident.

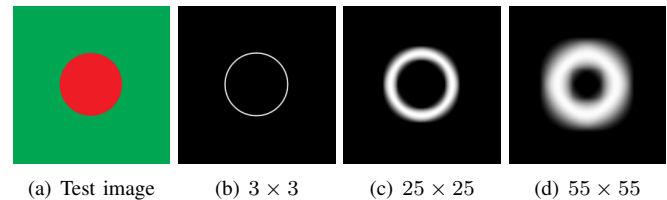


Fig. 2. The external energy computed at various scales (window sizes) for the synthetic test image.

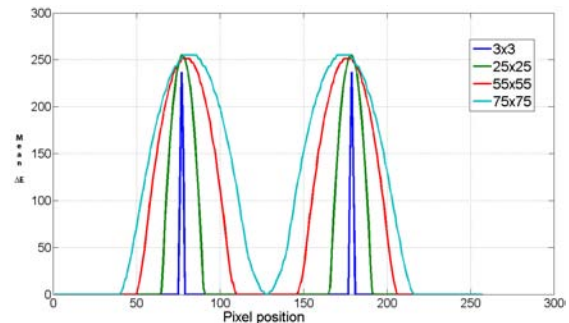


Fig. 3. Sections of the energy surfaces in Figure 2 at various scales.

Using the framework described in Section III, we simulated the segmentation of a skin lesion on a synthetic multi-fractal color texture image, using the model of color Brownian motion presented in [17]. The synthetic image is exhibiting two regions of different complexity: one texture is simpler (color fractal dimension = 2.23), corresponding to the background and implicitly to the healthy skin, and one texture more complex (color fractal dimension = 3.84), corresponding to the object to be segmented (the disc in the center of the image) - the skin lesion in our case of medical images. The border between the disc and the background is difficult to segment using the widely-used segmentation techniques: JSEG [18], watershed [19], pyramidal decomposition [20] (see Figure 4), compared against the results of our approach. In our experiments we used the implementations publicly available, either provided by authors (e.g. JSEG) or from the Intel OpenCV library. One may argue that for the mentioned segmentation approaches the final results strongly depend on the choice of input parameters (color distances, number of colors), but the results were unsatisfactory for a wide range of input values. The high complexity of the disc region determines the active contour not to stop on the border, but to keep advancing as the calculations of the total energy indicate that there might be an edge inside the complex texture. In this way, we simulated the barely visible edges between a skin lesion and the healthy skin. Figure 5 shows the initial, intermediate and final contours, as well as two energy surfaces – diffusions at two different scales.

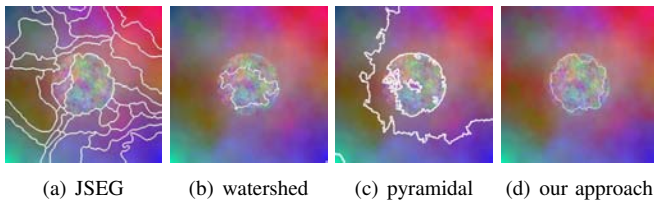


Fig. 4. Segmentation results using various approaches.

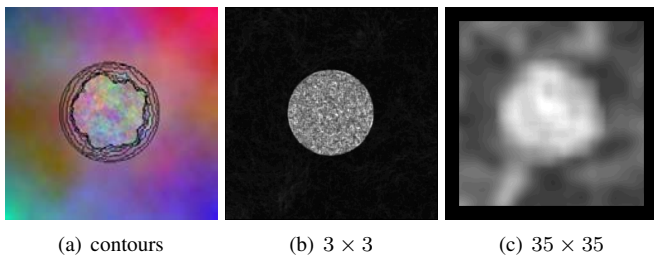


Fig. 5. Results on a synthetic color multi-fractal image.

V. EXPERIMENTAL RESULTS

In this section we present the results of the presented multi-resolution active contour approach using our proposed color diffusion model for several medical images of melanoma. Figures 6 and 7 illustrate the results obtained for a melanoma image when using two types of initialization.

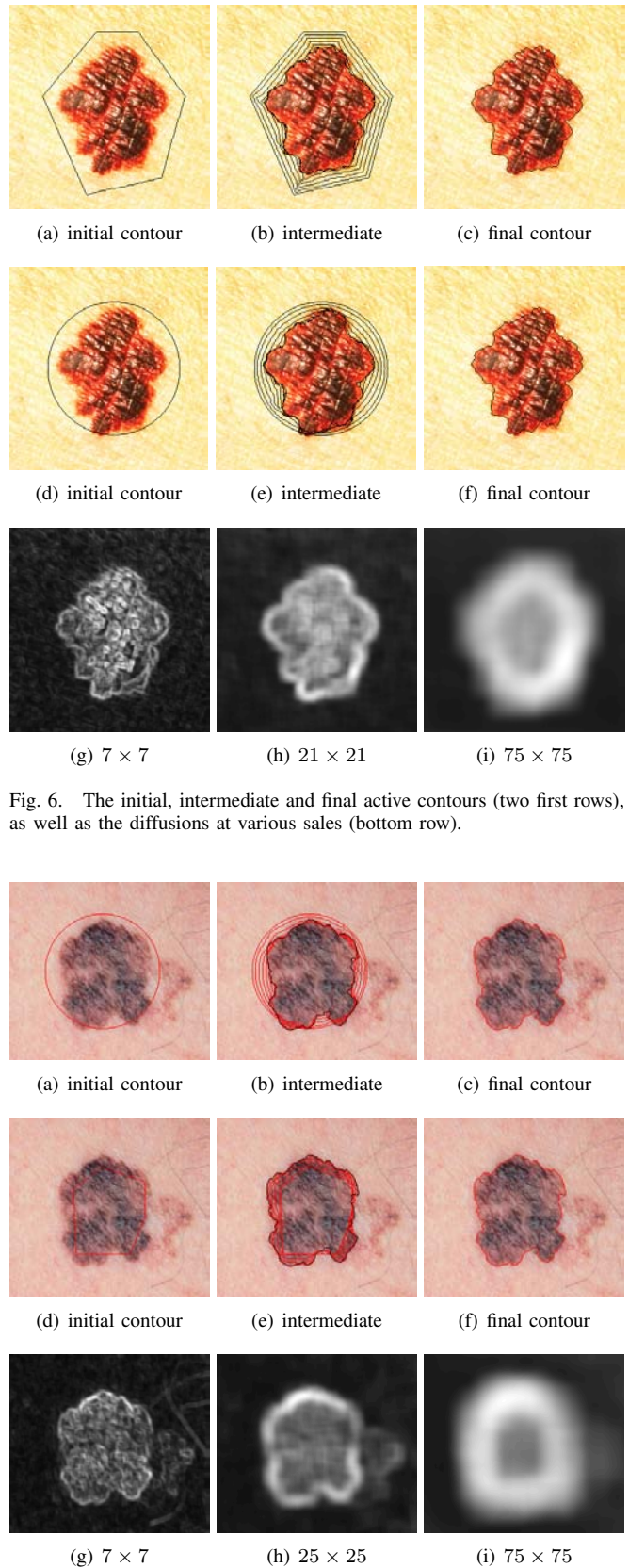


Fig. 6. The initial, intermediate and final active contours (two first rows), as well as the diffusions at various scales (bottom row).

Fig. 7. The initial, intermediate and final active contours (two first rows), as well as the diffusions at various scales (bottom row).

When dealing with this type of color medical images of skin lesions, from our experiments we conclude that it is

better to place the initial contour outside the skin lesion area, because if placed inside the lesion area it may be attracted by various strong inner edges leading to an unsatisfactory result. Further results are presented in Figure 8.

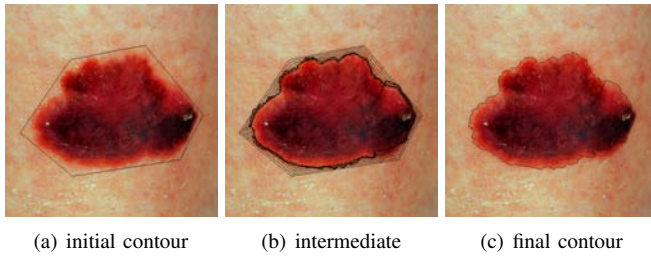


Fig. 8. The initial, intermediate and final active contours.

As expected, for an active contour approach the result of segmentation strongly depends on initialization of the contour - how far is it from the object of interest and what's its shape. Figure 9 shows an unsatisfactory result for the final position of the active contour when some of the points remained close to their initial position. The cause is the brownish/reddish area in the right of the lesion of interest, represented in the diffusion images as well (Figure 7), which attracts the active contour at a certain iteration. The active contour moves according to a Greedy algorithm which may get stuck in local extrema, so the brownish/reddish area keeps the active contour locked in that position, despite the fact that the border we want to detect is more visible.

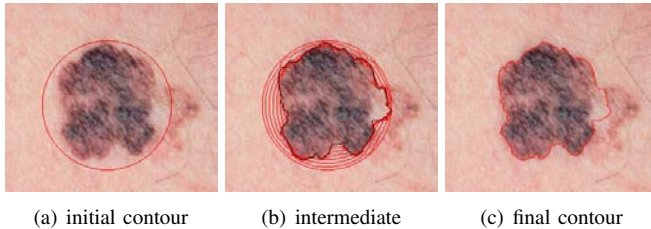


Fig. 9. The initial, intermediate and final active contours for an unsatisfactory segmentation result.

VI. CONCLUSIONS

We propose a diffusion model for color images to be used as external energy for active contours. It is based on the first-order moment of the correlation integral expressed using the CIE Lab ΔE distance between pixel colors. The active contour framework that we used is a multi-resolution approach based on the mean ΔE value computed locally, in windows of various sizes, capable to drive the active contour to the edges of the object to be segmented in a color image. We validated the model on synthetic multi-fractal color texture images, as well as natural textured images representing melanoma and psoriasis skin lesions. The active contour framework was implemented in MATLAB, but for a reasonably-fast implementation of the proposed diffusion model we preferred a parallel implementation on GPUs [21]. The measured time performance improvement showed an

acceleration factor of $200\times$, leading to a total running time of approximately one minute for an image of 400×400 pixels. We conclude that our approach could be used in a clinical screening application as preprocessing for melanoma ABCDE evaluation or psoriasis PASI score computation.

REFERENCES

- [1] Michael Kass, Andrew Witkin, and Demetri Terzopoulos, "Snakes: Active contour models," *International Journal of Computer Vision*, vol. 1, no. 4, pp. 321–331, 1988.
- [2] Ajit Singh, Demetri Terzopoulos, and Dmitry B. Goldgof, *Deformable Models in Medical Image Analysis*, IEEE Computer Society Press, Los Alamitos, CA, USA, 1st edition, 1998.
- [3] D. Terzopoulos, "Deformable models: Classic, topology-adaptive and generalized formulations," in *Geometric Level Set Methods in Imaging, Vision, and Graphics*, S. Osher and N. Paragios, Eds., chapter 2, pp. 21–40. Springer-Verlag, New York, 2003.
- [4] Chenyang Xu and Jerry L. Prince, "Snakes, shapes, and gradient vector flow," *IEEE Transactions on Image Processing*, vol. 7, no. 3, pp. 359–369, 1998.
- [5] Andrew P. Witkin, "Scale-space filtering," in *International Joint Conference on Artificial Intelligence*, 1983, pp. 1019–1022.
- [6] Andrew Witkin, Demetri Terzopoulos, and Michael Kass, "Signal matching through scale space," *International Journal of Computer Vision*, vol. 1, pp. 133–144, 1987.
- [7] I. Herlin B. Leroy and L. D. Cohen, "Multi-resolution algorithms for active contour models," in *12th Int. Conf. Analysis and Optimization of Systems*, 1996, pp. 58–65.
- [8] Laurent D. Cohen, "On active contour models and balloons," *CVGIP: Image Underst.*, vol. 53, pp. 211–218, March 1991.
- [9] Isaac Cohen Laurent D. Cohen, "Finite-element method for active contour models and balloons for 2-d and 3-d images," *IEEE Transactions on pattern analysis and machine intelligence*, vol. 15, no. 11, 1993.
- [10] K. P. Ngoi and J. C. Jia, "A new colour image energy for active contours in natural scenes," *Pattern Recognition Letters*, vol. 17, pp. 1271–1277, 1996.
- [11] A. Maalouf, P. Carre, B. Augereau, and C. Fernandez-Maloigne, "Foveal wavelet-based color active contour," in *Image Processing, 2007. ICIP 2007. IEEE International Conference on*, 16 2007-oct. 19 2007, vol. 1, pp. 1–245–I–248.
- [12] HaiJun Wang, Ming Liu, and WenLai Ma, "Color image segmentation based on a new geometric active contour model," in *Machine Vision and Human-Machine Interface (MVHI), 2010 International Conference on*, april 2010, pp. 6–9.
- [13] Silvano Di Zenzo, "A note on the gradient of a multi-image," *Comput. Vision Graph. Image Process.*, vol. 33, no. 1, pp. 116–125, Jan. 1986.
- [14] Peter Grassberger and Itamar Procaccia, "Measuring the strangeness of strange attractors," *Physica D: Nonlinear Phenomena*, vol. 9, no. 1–2, pp. 189–208, 1983.
- [15] Jean-Marc Bardet, "Dimension de corrlation locale et dimension de hausdorff des processus vectoriels continus - local correlation dimension and hausdorff dimension of continuous random fields," *Comptes Rendus de l'Acadmie des Sciences - Series I - Mathematics*, vol. 326, no. 5, pp. 589–594, 1998.
- [16] Madalina Turiac, Mihai Ivanovici, Tiberiu Radulescu, and Vasile Buzuloiu, "Variance-driven active contours," in *IPCV, 2010*, pp. 83–86.
- [17] M. Ivanovici and N. Richard, "Fractal dimension of colour fractal images," *IEEE Transactions on Image Processing*, vol. 20, no. 1, pp. 227–235, 2011.
- [18] Y. Deng, B. S. Manjunath, and H. Shin, "Color image segmentation," in *Proc. IEEE Computer Society Conference on Computer Vision and Pattern Recognition CVPR'99*, Fort Collins, CO, Jun. 1999, vol. 2, pp. 446–51.
- [19] S. Beucher, "Watersheds of functions and picture segmentation," may 1982, vol. 7, pp. 1928–1931.
- [20] Azriel Rosenfeld, *Some pyramid techniques for image segmentation*, pp. 261–271, Springer-Verlag, London, UK, 1986.
- [21] Zoltan Gaspar, Diana Stoica, and Mihai Ivanovici, "Colour diffusion model acceleration on gpus," in *OPTIM 2012 - 13th International Conference on Optimization of Electrical and Electronic Equipment*, Braşov, România, 2012, pp. 1429–1435.